Available online at www.sciencedirect.com
SCIENCE DIRECT®
Journal of Non-Crystalline Solids 351 (2005) 280–287
JOURNAL OF NON-CRYSTALLINE SOLIDS
www.elsevier.com/locate/jnoncrysol

Temperature dependence of the tribological properties of laser re-melted Al–Cu–Fe quasicrystalline plasma sprayed coatings

L.P. Feng [a,*], T.M. Shao [a], Y.J. Jin [a], E. Fleury [b], D.H. Kim [c], D.R. Chen [a]

[a] State Key Laboratory of Tribology, Tsinghua University, Beijing 100084, People's Republic of China
[b] Korea Institute of Science and Technology, Seoul 130-650, Korea
[c] Center for Noncrystalline Materials, Yonsei University, Seoul 120-749, Korea

Received 16 February 2004
Available online 15 December 2004

Abstract

The aim of this study was to investigate the effect of temperature on tribological properties of plasma-sprayed Al–Cu–Fe quasicrystal (QC) coating after laser re-melting treatment. The laser treatment resulted in a more uniform, denser and harder microstructure than that of the as-sprayed coatings. Tribological experiments on the coatings were conducted under reciprocating motion at high frequency in the temperature range from 25 to 650 °C. Remarkable influence of temperature on the friction behavior of the coating was recorded and analyzed. Microstructural analysis indicated that the wear mechanisms of the re-melted QC coatings changed from abrasive wear at room temperature, to adhesive wear at 400 °C and severe adhesive wear at 650 °C owing to the material transfer of the counterpart ball. It was also observed that the ratio of the icosahedral (i)-phase to β-$Al_{50}(Fe,Cu)_{50}$ phase in the coating was higher after test at 400 °C than that at 650 °C. The variation of the ratio i/β of coating and of the property of the counterpart ball and coating with the temperature are the two main factors influencing the wear mechanisms and value of the friction coefficient.

PACS: 61.44.Br; 42.62.Cf; 52.77.Fv; 46.55.+d

1. Introduction

Many fundamental and application studies have been performed on quasicrystals (QC) since Shechtman observed in a TEM an aperiodic diffraction pattern with five-fold symmetry in 1984 [1–5]. Nowadays, engineers are investigating potential applications, which could benefit from the combination of good properties such as high hardness, low surface energy, low thermal and electrical conductivities and good corrosion properties [6–11]. The intrinsic brittleness of QC materials at temperature lower than $0.6T_m$ (T_m = melting temperature) limits their industry application. However, at high temperature, QC materials exhibit interesting properties such as superplasticity etc. Although stable quasicrystals could form in some alloy systems, for instance Al–Cu–Fe system, the majority of quasicrystalline phases are metastable [12]. High quenching rates are, in general, necessary to produce these quasicrystalline phases, and rapid solidification techniques, such as melt spinning [13] and thermal deposition, have been used to produce quasicrystals, in the form of thin ribbons and coatings, respectively. Plasma spray is particularly appropriate for the preparation of coatings containing a high fraction of i-phase [14,15], but the drawback of this technique is the inferior microstructure features such as interlamellar and pores (due to imperfect contact and partially molten particles), intra- and inter-splat

* Corresponding author. Present address: State Key Laboratory of Nonlinear Mechanics, Institute of Mechanics, Chinese Academy of Sciences, Beijing 100080, People's Republic of China. Tel.: +86 10 62783160; fax: +86 10 62781379.
E-mail address: fenglp@263.net (L.P. Feng).

0022-3093/$ - see front matter © 2004 Elsevier B.V. All rights reserved.
doi:10.1016/j.jnoncrysol.2004.08.269

microcracks (due to stress relaxation) and splat boundaries generally observed in the coatings. These features greatly influence the physical and mechanical properties such as the thermal conductivity, elastic modulus, strength, fracture toughness and thus reduce their performances [16,17].

Laser surface treatment techniques provide wide ranges of interesting solutions to enhance the wear and corrosion resistance of surface layers made of either metallic or ceramic materials [18]. In a recently study, an attempt was made to treat the surface of plasma sprayed QC coating by laser re-melting technique, and results indicated that the laser treatment increased the content of the icosahedral phase, owing to the large temperature gradient and high cooling rate in the laser melting pool, which consequently enhanced the property of the coating layers [19].

In the last ten years, friction and wear properties of quasicrystaline Al–Cu–Fe alloys were investigated at low and moderate temperature [20,21]. Although it was suggested that QC materials could be potentially useful at high-temperature, to the authors' knowledge the tribological properties of QC materials have not been investigated at temperature higher than 450 °C [22,23]. The aim of this work was to investigate the effect of laser re-melting on the structure of the plasma sprayed coatings and the influence of the temperature on the friction behavior and wear mechanisms of the laser treated coatings.

2. Experimental details

2.1. Coating preparation

Gas atomized powder with a nominal composition of $Al_{62}Cu_{26}Fe_{12}$ was used in this study. The powder with size of −200 to +400 meshes (38.1–73.9 μm) was deposited in air onto the surface of medium carbon steel disc (0.45 wt% C, 0.65 wt% Mn and 0.2 wt% Si) using a METCO-type plasma spray gun. The disc is ∅24 mm with 10 mm thickness and a surface roughness of Ra = 1.6 μm. The parameters used for plasma spraying were listed in Table 1. The thickness of sprayed coating was approximately 0.35 mm. Then the coating was re-treated by laser re-melting technique. A YAG continuous solid laser was used and the processing parameters were: laser power $P = 260$ W, scanning velocity $V = 4$ mm/s, beam diameter $D = 0.5$ mm, yielding a energy density, P/VD, of about 130 J/mm^2. Argon gas with a flux of 5.0 l/min was used as shielding gas to protect the melting pool from oxidation.

Table 1
Operating parameters for plasma spray

Parameter	Set-up value
Arc current	600 A
Primary gas (Ar) flow rate	160 l/min
Secondary gas (H_2) flow rate	9 l/min
Powder feeding rate	110 g/min
Spraying distance	20 mm
Gun displacement rate	Put an approximate value (manual)

2.2. Tribological tests

Tribological tests of QC coatings were performed with a ball on disk SRV friction and wear test machine under reciprocating motion. A standard ball of 12.7 mm in diameter, made of GCrl5 steel (1 wt% C, 0.3 wt% Mn and 1.5 wt% Cr) with a hardness of HV742, was pressed with a reciprocating motion on the fixed disc with laser re-melted QC coating. The coating was polished and ultrasonic cleaned in acetone before tribological test. The initial surface roughness of the coating was 0.3 μm. During the test, the temperature was increased from 50 °C to 650 °C with step of 50 °C. The friction coefficient, automatically calculated from the ratio of the mean value of the friction force in one stroke to the normal load, was recorded together with the frequency and applied normal load. In present study, the normal load was 10 N, the reciprocating stroke, S, was 0.6 mm, and the frequency was taken as 50 Hz. All the tests were carried out under non-lubrication condition in air. A DM-400 microindenter operating at 100 N load with pressed time of 15 s was used for measuring the microhardness of the coatings.

2.3. Coating characterization

An optical microscope and an SEM with EDX analysis systems were employed for the microstructural characterization and the local phase composition analysis after etching with Keller's reagent. An X-ray diffractometer using a Cu Kα radiation and a Ni filter was used to identify the phases of the coating. A stylus profilometer was used to measure the roughness of the surfaces of the worn scar. Wear debris was also collected during wear testing and was then examined under SEM to complement the analysis of wear mechanisms.

3. Results and discussion

Fig. 1 shows optical micrographs of the plasma sprayed coating surface before and after laser re-melting. In the as-spray state, the microstructure of the coating layer was non-uniform, as coatings are built-up from the flattening and solidification of individual droplets [22,24]. The coating was rather loose, with liquefied droplets flatted on the substrate, pores and deformed particles distributed in the coating (Fig. 1(a)), resulting

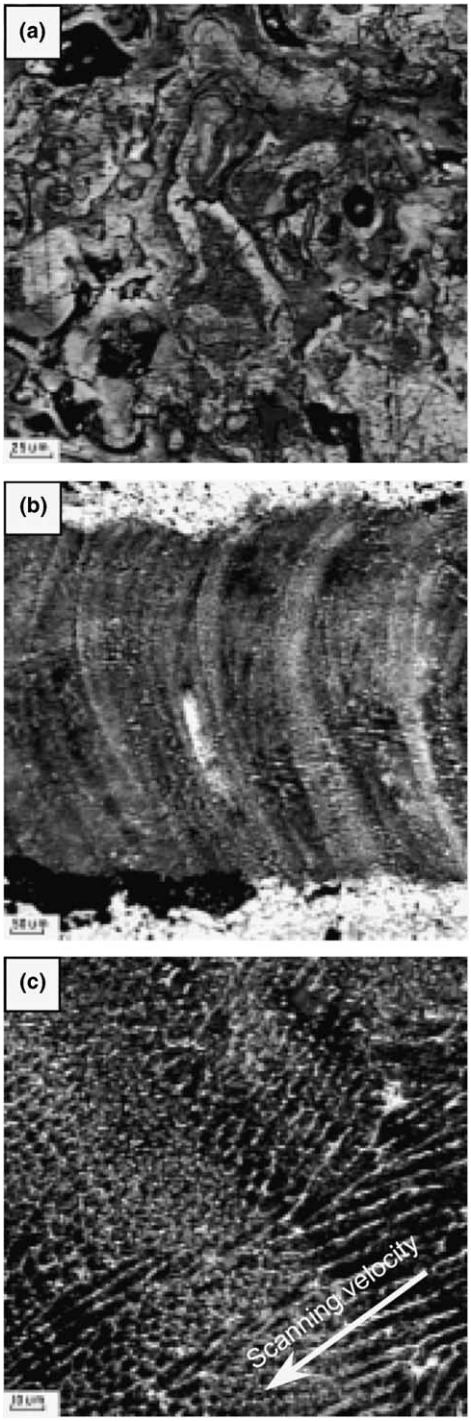

Fig. 1. Surface view showing the morphology of (a) primary AlCuFe quasicrystalline plasma sprayed coating, (b) laser re-melted plasma sprayed zone and (c) higher magnification of the local area of the laser treated sample.

in the typical features of plasma sprayed coatings [15]. Low values of the microhardness, about Hv251, were obtained. In Fig. 1(b), the laser treated trace with a width of 0.6 mm can be observed in the middle part of the photograph. The average microhardness value of the laser re-melted coating was equal to Hv744, which is a typical value reported for cast Al–Cu–Fe alloys and approximately three times of that of plasma sprayed coating [24,25]. The laser-remelted coating has a uniform structure. A higher magnification view (Fig. 1(c)) of the laser treated zone of the plasma sprayed coating indicates that the pores and deformed particles of the coating were almost eliminated. Furthermore, the dendrites are rather thin and dense, with the orientation of the dendrites almost parallel to the scanning velocity. Due to the anisotropy of properties such as the solid–liquid interface energy and growth kinetics, dendrite stems grow preferentially along the crystallography directions closest to the direction of heat flow [26,27]. In these experiments, the heat flow on the top of the melting pool was almost parallel to the scanning velocity so the dendrite stalks were parallel to the scanning velocity. The primary arm spacing was about 5um, which is in the range of super-fine dendrites [28]. The appearance of the super-fine dendrites resulted from the high temperature gradient and solidification velocity in the melting pool.

The i-phase in the Al–Cu–Fe alloy system forms in an extremely narrow domain in the equilibrium phase diagram and is usually accompanied by several other crystalline and approximant phases, if the composition and solidification behavior are not strictly controlled [29]. Laser re-melting is a suitable technique to obtain coatings containing a large volume fraction of i-phase owing to the high temperature gradient and solidification velocity in the laser melting pool. Influences of processing parameters of laser re-melting on the phase in the plasma sprayed coatings were previously investigated. Results indicated that for the energy density larger than 16 J/mm^2, the main phases in the coating were β-$Al_{50}(Fe,Cu)_{50}$ and icosahedral (i)-phases. The ratio of i/β varied with the increase of energy density [19]. In this work, the energy density was about 130 J/mm^2,

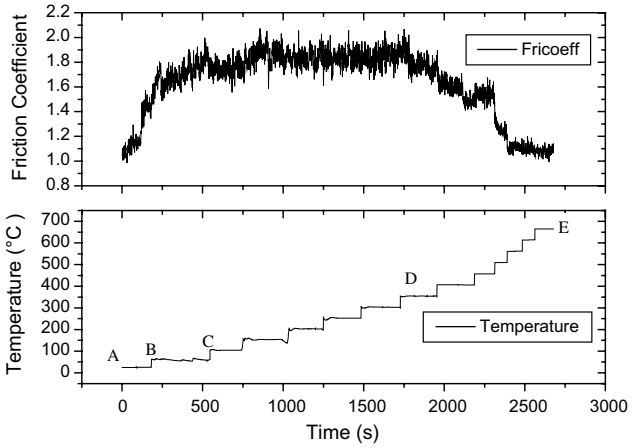

Fig. 2. Variation of the coefficient of friction with the temperature.

so it can be deduced that the phases in the coating at room temperature are the i and β-phases, too.

Fig. 2 shows the variation of the friction coefficient of the coating with temperature. These variations can be divided into four distinct stages: in the run-in stage at room temperature (AB), the friction coefficient increases from 1.0 to 1.5. From around 50–150 °C (BC), the friction coefficient increased and reached to a maximum (near 2.08) at 150 °C. Between 150 °C and 350 °C (CD), the coefficient of friction remained constant then exhibited a step decrease down to 1.2 between 350 °C and 550 °C (DE). From 550 °C and up to 650 °C, the coefficient of friction keeps stable once again.

Figs. 3 and 4 show the morphologies of worn surface of the laser treated coating and of counterpart ball, respectively, after tests at room temperature, 400 °C and 650 °C. At room temperature, thin worn traces on the coating surface were clear and wear particles can

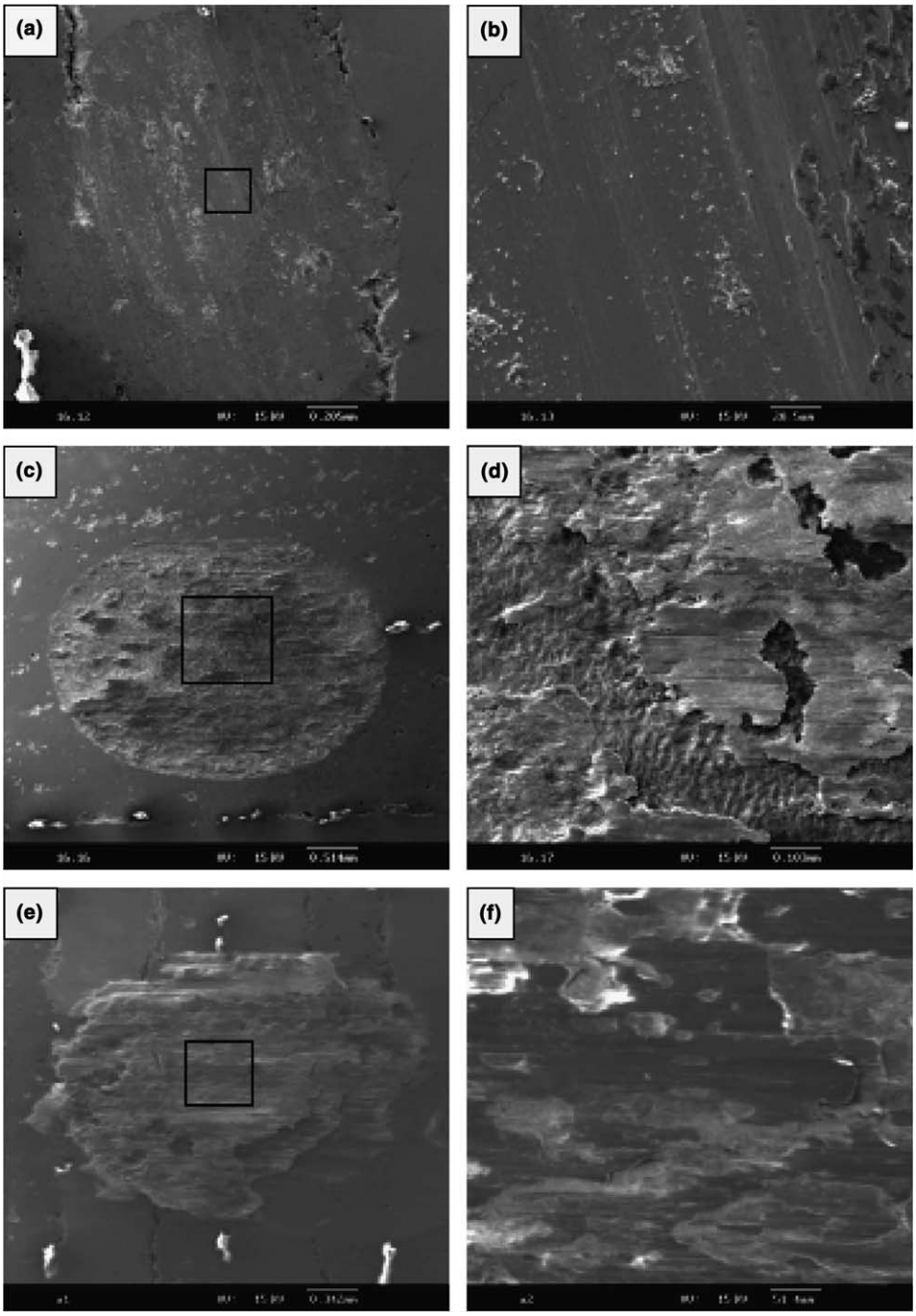

Fig. 3. Morphologies of the wear scar on the coating after test (a) at room temperature, (c) at 400 °C and (e) at 650 °C; (b), (d) and (f) are the magnified view of (a), (c) and (e), respectively.

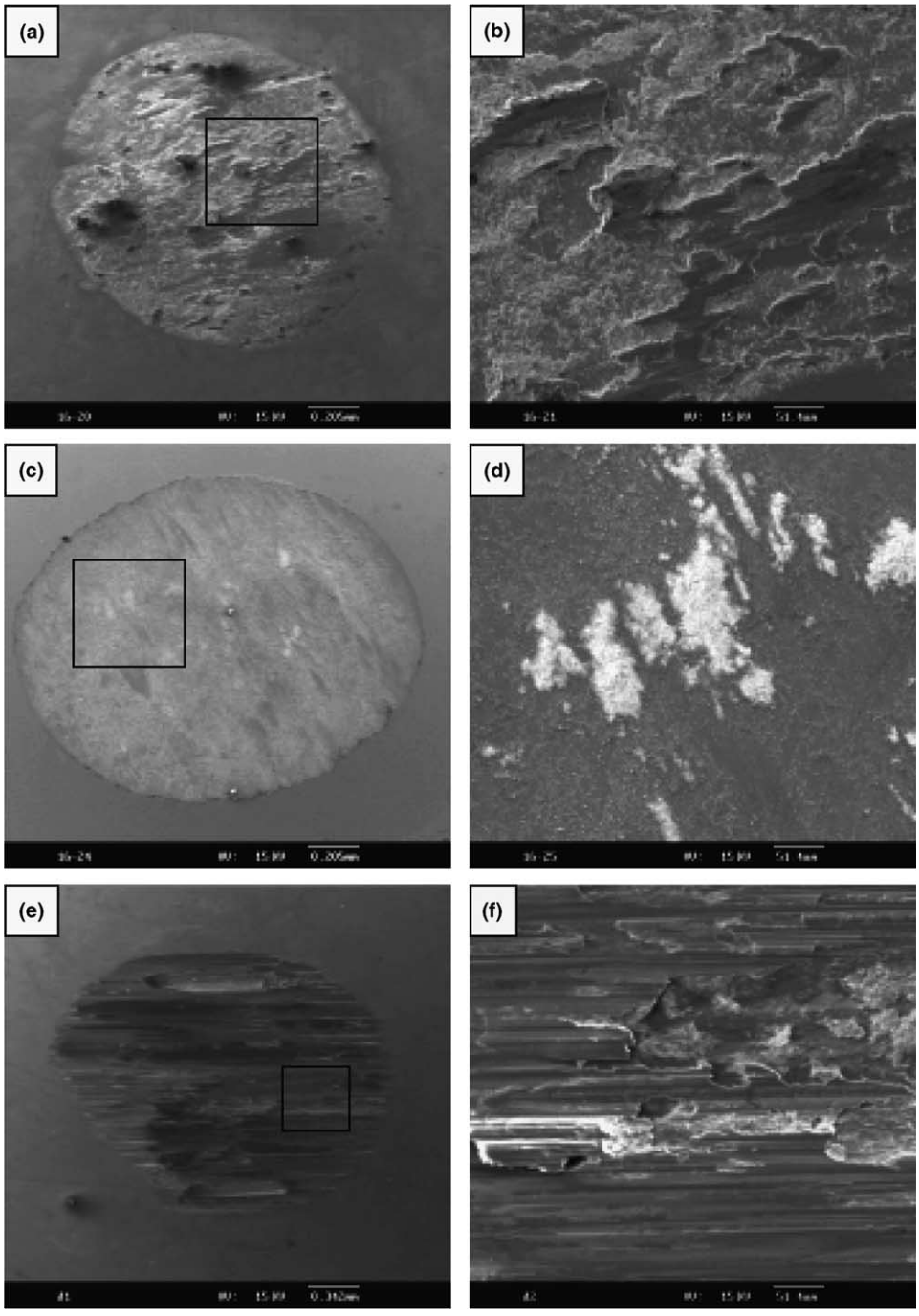

Fig. 4. Morphologies of the wear scar on the counterpart ball after test (a) at room temperature (c) at 400 °C and (e) at 650 °C; (b), (d) and (f) are the magnified view of (a), (c) and (e), respectively.

clearly be distinguished (Fig. 3(a)). Because of the intrinsic brittleness of Al–Cu–Fe quasicrystal material of the coating, the dominant wear mechanism was abrasive wear. Local spallation occurred on the surface of the counterpart ball (Fig. 4(a) and (b)). Many of these plate-type particles, which accumulated and adhered on the surface coating, are believed to be responsible for the acceleration of the abrasive wear of the counterpart ball. Although values of the microhardness of the counterpart ball and the coating were similar, the extent of wear on the counterpart ball was found to be more severe than that of the coating. During friction tests, the plastically deformed particles accumulated at the contact region and then transferred onto the counterpart ball, increasing the surface roughness and changing the nature of the contact. This was the main factor that leads to the increase of friction coefficient at room temperature.

At 400 °C, flat patches scattered on the worn surface of the laser treated coatings (Fig. 3(c) and (d)). EDX measurements indicated that main elements in the patches were O and Fe with a little amount of Al. The patches were thus mainly composed of the plastically deformed materials from the couple ball. Consequently, the wear mechanism of the laser coating in this range of temperature was a combination of adhesive and oxide wear. For the couple ball, the worn scar is obvious and deep, and several white products distributed on it (Fig. 4(c) and (d)). EDX results showed that the white ones corresponded to Fe oxides. The wear damage was rather large in comparison to that at room temperature. The change of the worn mechanism may be one factor that resulted in the higher value of the friction coefficient at around 400 °C than that at room temperature.

After friction experiment at 650 °C, the wear scar of the coating was covered by a flat layer and the damage of the coating was not obvious (Fig. 3(e) and (f)). Serious worn happened on the counterpart ball and the materials were peeled off laceratedly (Fig. 4(e) and (f)). As shown in Fig. 5, wear particles seem to agglomerate together. EDX analyses of coating, counterpart ball and debris at 650 °C are given in Table 2. On both of the coating and counterpart ball, elements O, Si, Cr and Fe were detected, which indicate that part of the counterpart ball was worn off and transferred onto the coating surface, and that oxides of Cr and Fe formed. It can easily be deduced from these microstructural observations that particles from the counterpart ball were firstly detached and transferred onto the contact surface, then were plastically flattened owing to the continuous reciprocating movement of the counterpart ball on the coating. Furthermore, it is well known that, in steel, the α-phase transforms into the γ-phase above 550 °C, according to the phase diagram of Fe–C alloy. Thus properties such as shear strength and hardness of the counterpart ball are reduced, which results in the decrease of the wear resistance. Another evidence for the material transfer is the fact that the composition of the wear particles contains Si, Cr, Fe and a little Al, indicating the severe wear of the counterpart ball and a relatively lower damage of the coating surface.

Table 2
Element composition on coating, counterpart ball and wear particles (wt%)

Elements	O	Al	Si	Cr	Fe
Coating	25.36	–	0.34	0.80	73.15
Counterpart ball	21.40	–	0.12	1.31	77.17
Wear particles	22.39	0.65	0.22	1.00	75.74

Fig. 5. Morphologies of the wear particles.

Fig. 6(a) and (b) show the surface topography of the wear scars of the coatings after tests at room temperature and 650 °C, respectively, which correspond to the SEM images shown in Fig. 3(a) and (c), respectively. In these figures, the wear scar is concave at room temperature, indicating the wearing-off of the coating material, but is convex with teeth-like in some places at 650 °C, showing a detachment and adhesion of material from the counterpart ball onto the coating surface.

XRD traces of the coatings after tests at 400 °C and 650 °C are shown in Fig. 7(a) and (b), respectively. At these two temperatures, both i-phase and β-phase could

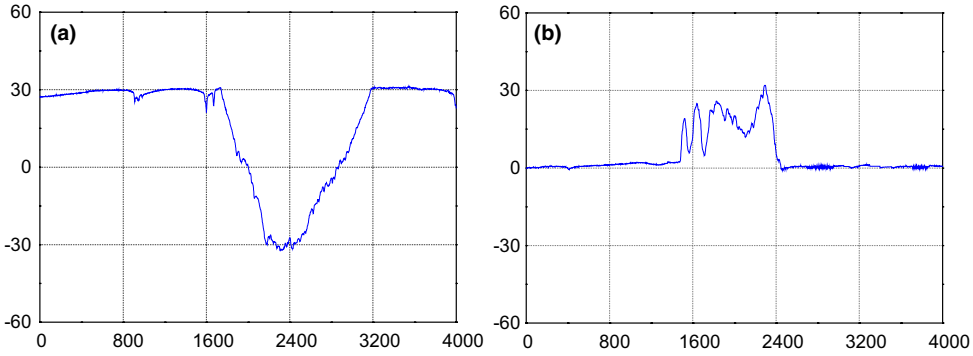

Fig. 6. Surface morphologies of the wear scar after test performed (a) at room temperature and (b) at 650 °C.

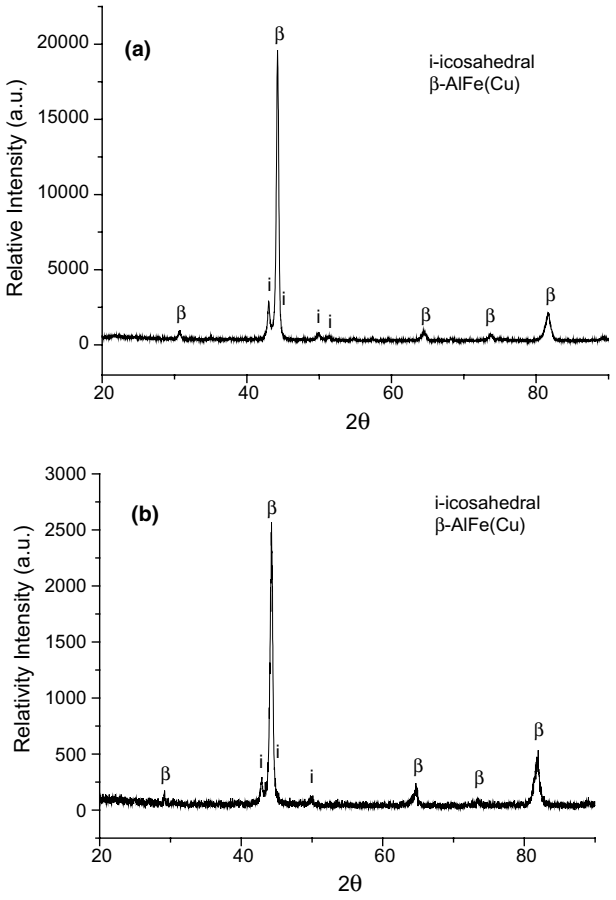

Fig. 7. XRD results of the coating after test (a) at 400 °C and (b) at 650 °C.

be detected on the surface of the coating, and the i/β ratio of the coating after test at 650 °C is smaller than that at 400 °C. The i-phase in the Al–Cu–Fe coating is thermodynamically stable up to 860 °C. The reduction of i-phase was possibly resulted from the diffusion of element Fe from the substrate to the coating at 650 °C, the addition of which can destabilize the i-phase by shifting the composition toward the β-phase [30].

Four factors may influence the friction coefficient at around 650 °C. Firstly, the ratio of i/β decreased with the rising of temperature, which caused the increase of friction coefficient. Secondly, the formation of an oxide Cr film on the counterpart ball surface, which may decrease the friction coefficient of the material, as suggested by other studies [31,32]. Thirdly, the shearing strength and hardness of the QC coating and counterpart ball decreased with the increase of temperature. Finally, the ductility and plasticity of Al–Cu–Fe increased above 600 °C [33] and should result in the enhancement of the wear resistance, thus reducing the amount of wear particles produced by abrasive wear. From previous experiments, it is believed that the first mechanism led only to a moderate change of the coefficient of friction [17]. Most experiments on engineering materials have shown that the friction coefficient increased with the rising of temperature, but decreased at rather high temperature. Thus, the decrease of the coefficient of friction at high temperature is attributed to the softening of both the coating layer and the counterpart materials.

4. Conclusion

Al–Cu–Fe quasicrystalline plasma-sprayed coatings were treated using laser re-melting technique. The microstructure of the laser treated coatings was denser and more uniform, and presented primary arm spacing of about 5 μm. The properties of the coating were also improved owing to the laser treatment. The average value of the Vickers microhardness was found to be about twice higher than that of the plasma-sprayed coating, and equivalent to that of as-cast alloy.

Tribological experiments of the laser re-melted plasma sprayed coating were carried out on a SRV instrument in the temperature range from room temperature to 650 °C. Both the friction behavior and wear mechanism were found to be dependent on temperature. The friction coefficient increased from 1.0 to 1.5 at room temperature to reach a peak value of around 2.08 at 150 °C, then remained stable up to 350 °C and then exhibited step change down to 1.2 till 550 °C and kept stable once again from 550 °C to 650 °C. With the increase of the temperature, a transition of the wear mode was observed from abrasive wear at room temperature, to adhesive wear combined with oxide at 400 °C and severe adhesive wear caused by material transfer of the counterpart ball at 650 °C.

Acknowledgments

This work was supported by National Natural Science Foundation of China No. 50075042 and Postdoctoral Foundation of China No. 2003034143. D.H. Kim is grateful for the financial support by the Creative Research initiatives of the Korean Ministry of Science and Technology.

References

[1] D. Shetchman, I. Blech, D. Gratias, J.W. Cahn, Phy. Rev. Lett. 53 (1984) 1951.
[2] J.M. Dubois, S.S. Kang, J. von Stebut, J. Mater. Sci. Lett. 10 (1991) 537.
[3] Y.L. Cheung, K.C. Chan, Y.H. Zhu, Materials Characterization 47 (2001) 299.
[4] B. Wolf, K.O. Bambauer, P. Paufler, Mat. Sci. Eng. A 298 (2001) 284.
[5] J.M. Dubois, Mat. Sci. Eng. A 294–296 (2000) 4.
[6] U. Köster, W. Liu, H. Liebertz, M. Michel, J. Non-Cryst. Solids 153&154 (1993) 446.

[7] P. Brunet, L.M. Zhang, D.J. Sordelet, M. Besser, J.M. Dubois, Mater. Sci. Eng. A 294–296 (2000) 818.
[8] P.A. Thiel, J.M. Dubois, Materials Today 2 (1999) 3.
[9] C.J. Jenks, P.A. Thiel, Mater. Res. Bull. 11 (1997) 55.
[10] T.M. Shao, X.K. Cao, E. Fleury, D.H. Kim, M. Hua, D. Se, J. Non-Cryst. Solids 334&335c (2004) 466.
[11] F. Gayle, A. Shapiro, F. Biancaniello, W. Boettinger, Metall. Trans. A 23A (1992) 2409.
[12] M.F. Besser, T. Eisenhammer, MRS Bull. 11 (1997) 59.
[13] E. Shield, J.A. Campbell, D.J. Sordelet, J. Mat. Sci. Lett. 16 (1997) 2019.
[14] E. Fleury, S.M. Lee, W.T. Kim, D.H. Kim, J. Non-Cryst. Solids 278 (2000) 194.
[15] Z. Wang, A. Kulkarni, S. Deshpande, T. Nakamura, H. Herman, Acta Mater 51 (2003) 5319.
[16] W.D. Yuan, T.M. Shao, E. Fleury, D. Se, D.R. Chen, Surface & Coating Technology 185 (2004) 99.
[17] D.J. Sordelet, M.F. Besser, J.L. Logsdon, Mat. Sci. Eng. A 225 (1998) 54.
[18] J. Kusinski, Applied Surface Science 86 (1995) 317.
[19] W.D. Yuan, T.M. Shao, D. Se, D.R. Chen, Material Engineering 11 (2002) 7 (in Chinese).
[20] S.S. Kang, J.M. Dubois, J. Mater. Res. 8 (10) (1993) 2471.
[21] X.Y. Zhou, J.M. Luo, R.G. Wan, Tribology 22 (2002) 232 (in Chinese).
[22] E. Fleury, S.M. Lee, J.S. Kim, W.T. Kim, D.H. Kim, H.S. Ahn, Wear 253 (2002) 1057.
[23] E. Huttunen-Saarivirta, Journal of Alloys and Compounds 363 (2004) 150.
[24] K.H. Baik, P.S. Grant, B. Cantor, Acta Mater 52 (2004) 199.
[25] E. Giacometti, N. Baluc, J. Bonneville, J. Rabier, Scripta Materialia 41 (1999) 989.
[26] R. Trivedi, W. Kurz, Int. Mater. Rev. 39 (1994) 49.
[27] W. Kurz, R. Trivedi, Mater. Sci. Eng. A 179 (1994) 46.
[28] L.P. Feng, W.D. Huang, Y.M. Li, H. Yang, X. Lin, Acta Metallurgica Sinica 38 (2002) 501 (in Chinese).
[29] L. Bresson, D. Gratias, J. Non-Cryst. Solids 153&154 (1993) 468.
[30] L.M. Zhang, R. Luck, Journal of Alloys and Compounds 342 (2002) 53.
[31] S.Z. Wen, P. Huang, Tribological Principle, Tsinghua University, Beijing, 2002, 302 (in Chinese).
[32] D.H. Buckley, in: N.P Suh, N. Saka (Eds.), Fundamentals of Tribology, MIT, Cambridge, MA, 1978, p. 53.
[33] K. Urban, M. Feuerbacher, M. Wollgarten, MRS Bull. 11 (1997) 65.